Acta Astronautica 170 (2020) 637–651

Contents lists available at ScienceDirect

Acta Astronautica

journal homepage: www.elsevier.com/locate/actaastro

Review article

Just in time collision avoidance – A review

Christophe Bonnal[a,*], Darren McKnight[b], Claude Phipps[c], Cédric Dupont[d], Sophie Missonnier[d], Laurent Lequette[d], Matthieu Merle[d], Simon Rommelaere[d]

[a] CNES-Launcher Directorate, 52 rue Jacques Hillairet, 75012, Paris, France
[b] Centauri, 15020 Conference Center Drive Chantilly, VA, 20151, USA
[c] Photonic Associates, LLC, 200A Ojo de la Vaca Road, Santa Fe, 87508, USA
[d] CT Paris, 41 Boulevard Vauban, 78280, Guyancourt, France

ARTICLE INFO

Keywords:
Orbital debris
Collision avoidance
COLA
Just in time collision avoidance
JCA
Space traffic management
STM
Space environment management
SEM
Active debris removal
ADR
Large debris traffic management
LDTM

ABSTRACT

The ever increasing number of orbital objects since 1957 raises numerous questions concerning future sustainability of space. Among the 34,000 objects larger than 10 cm in orbit, 20,000 only are cataloged. These cataloged objects include roughly 2000 active satellite, among which less than 1500 are maneuverable. All the rest are orbital debris, large satellites of launcher upper stages, mission related objects, inert pieces from fragmentations or collisions, with no maneuvering capabilities.

Collision Avoidance is a common practice when at least one maneuvering satellite is involved, even though it requires a very significant effort to do so.

But it is today not possible to avoid collisions among two debris, which represent by far the most frequent collision scenario. It appears necessary to find solutions to avoid such collisions as they have the potential to generate thousands of new orbital pieces and feed to so-called Kessler syndrome; indeed, numerous publications underline the frequent near-misses among very large derelict, and the consequences such collisions would have.

Several solutions for such "Just in time Collision Avoidance (JCA)" have been proposed and are recalled in the paper. Three of them have recently been studied in order to assess their feasibility, and appear promising.

The use of an orbital laser system can first drastically improve our the accuracy of the ephemerids, second impart a very small ΔV to a passive debris early enough to enable a significant increase in distance between the two objects.

Another solution which appears very promising considers the launch on a small sounding rocket of a system releasing a cloud of particle and gas in front of one of the debris; the associated drag, even very small, is enough to lower the probability of an announced collision.

Swarms of nano-tugs could also be attached to the most hazardous derelicts, de-tumble them, and slightly modify their trajectory in order to prevent collisions.

1. Context of just-in-time collision avoidance (JCA) operations

The ever-increasing number of space debris raises numerous concerns, casualty risk on ground following uncontrolled reentry, damage of operational satellites, or generation of large number of new debris following massive collisions.

Various actions can be considered to handle this space debris problematic, potentially summarized in the following diagram (Fig. 1), adapted from the one generally considered and widely published, initiated in Ref. [1]. The Space Situational Awareness branch (SSA) provides all the necessary data coming from Space Surveillance and Tracking (SST) and Space Weather. It can be used for spacecraft safety concerns, through Space Traffic Management (STM) or to help at aiming at long term sustainability of space through Space Environment Management (SEM) actions, first through mitigation, then through remediation actions, namely Active Debris Removal (ADR) and Just-in-time Collision Avoidance (JCA).

The general goal of this paper is to give an overview of the JCA actions currently under study.

This risk of major catastrophic collisions in orbit between two large non-maneuverable objects is the most critical for long term sustainability of space operations as it leads to a cascading effect, potentially

* Corresponding author.
E-mail addresses: Christophe.bonnal@cnes.fr (C. Bonnal), Darren.McKnight@centauricorp.com (D. McKnight), crphipps@aol.com (C. Phipps), cedric.dupont@ctingenierie.com (C. Dupont).

https://doi.org/10.1016/j.actaastro.2020.02.016
Received 5 February 2020; Accepted 8 February 2020
Available online 14 February 2020
0094-5765/

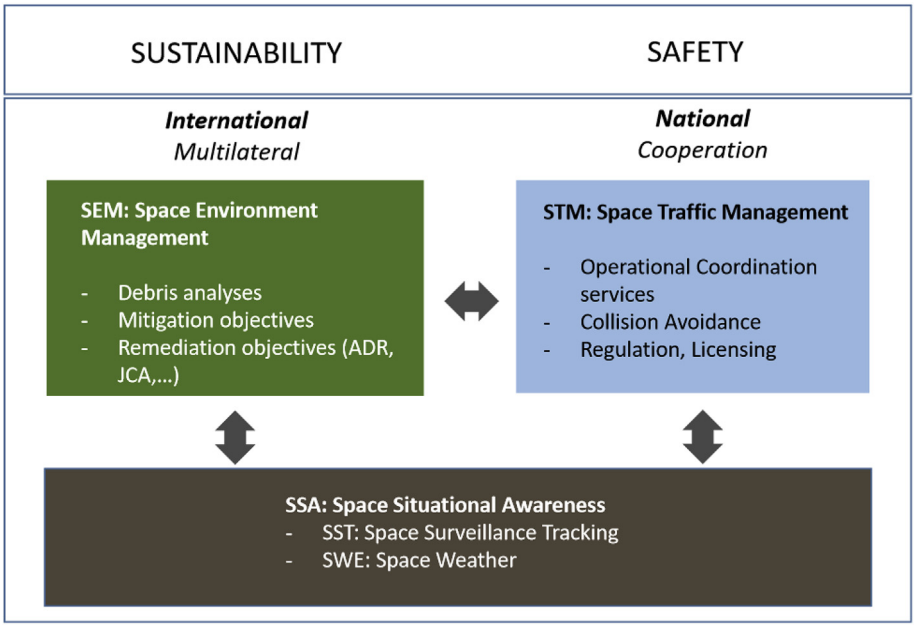

Fig. 1. Overall relation between debris related actions [CNES].

uncontrollable, known as the Kessler syndrome [2]. The problem comes from the fact that among the 20,000 large objects currently in the public catalog, 2000 only are operational, among which 1500 are maneuverable, 7.5% of the population, capable if necessary to perform an active collision avoidance maneuver.

Such Space Traffic Management (STM) actions are safety driven maneuvers, meant to protect our most important space assets, but by definition they can be performed only when one at least of the two objects is maneuverable; it means that 86% of the collisions among cataloged objects cannot be avoided today.

Among these potential collisions, more than half of them imply one very large non-maneuverable object as more than one third of the cataloged objects are old spacecraft and rocket bodies; one can recall that according to our collision models, it takes a debris of half a kilogram to shatter completely a 1-ton object, generating thousands of new debris.

The most critical debris have been identified, and a formalized approach is ongoing worldwide to quantify exhaustively the criticality of each large debris. Some zones are particularly well known, housing large clusters of large debris, mainly SL-8, SL-16 and associated payloads. These clusters have been extensively analyzed, mainly C775, C850 and C975 [3,4] (and more recently a new Cluster C615 [5]), the Fig. 2 giving the mean altitude.

McKnight has shown that the situation in these clusters is not sustainable: for instance, there is a passage in C850 of two SL-16 stages (9 tons) within 200 m distance every month; there is also an average collision rate of SL-8 (1.4 tons) in C975 of 1/90 per year. Such a collision would generate a very large number of new debris and trigger a situation which may turn out to be non-sustainable at medium to long term.

To counter these collisions among large objects, two approaches can be considered within SEM:

- The “strategic” one consists in retrieving a certain number of large debris each year, typically among these large clusters, thus reducing the probabilities of major collisions. This ADR strategy [6] has been intensively studied throughout the world for more than 10 years. It appears to be technically feasible, but hard to finance, and raises numerous non-technical problems such as legal or political ones. In addition, it would be quite useless as long as the mitigation rules, internationally agreed-upon, are not complied to in a much higher way; there is no use in going to deorbit a couple of large debris as long as we generate more of them continuously,
- The “tactical” one [7,8] is aimed at lowering the probability of a detected potential collision by acting on one of the two debris some time prior to the predicted collision date. This strategy is called JCA. The first ideas were presented some 10 years ago, and among the solutions which have been proposed, slightly slowing one of the debris via an impulsive drag force appears promising. For the tactical approach, flexibility and reactivity are, with the perennial cost criterion, the main challenges.

2. Accuracy of ephemerids of resident space objects

2.1. Typical requirements for future collision avoidance and JCA operations

The current typical accuracy of large debris orbits is in the order of ± 1 km along the velocity vector, ± 200 m radial and ± 300 m off-plane [9]; such values depend a lot on numerous parameters, size or Radar Cross Section, altitude, inclination or the orbit and revisit time with respect to SST sensors, but globally this accuracy is not good enough to guarantee an acceptable false-alarm ratio for STM, or to enable JCA actions. Colleagues from The Aerospace have shown that in the frame of the upcoming deployment of large constellations, “the tracking uncertainty on all objects, including dead satellites, and cataloged debris of all tracked sizes, may need to be on the order of meters in each axis” [9]. In a similar way, Krag shows the strong influence of orbit accuracy on the number of false alarms for Collision Avoidance, and sets the objective for an improvement by a factor 10 at least compared to the Conjunction Data Messages (CDM), which would represent a gain in terms of false alerts by a factor 50 [10].

2.2. Orbital ranging laser solution

We must be able to precisely determine the orbits of these objects as they become uncontrolled. To accomplish this, we propose an orbiting pulsed laser station with a high sensitivity, high data rate detector array to improve orbital center-of-mass range precision to 10 cm relative to the station (Fig. 3). Its detector array can also determine transverse location with 45 cm precision at 1000 km range and proportionally less

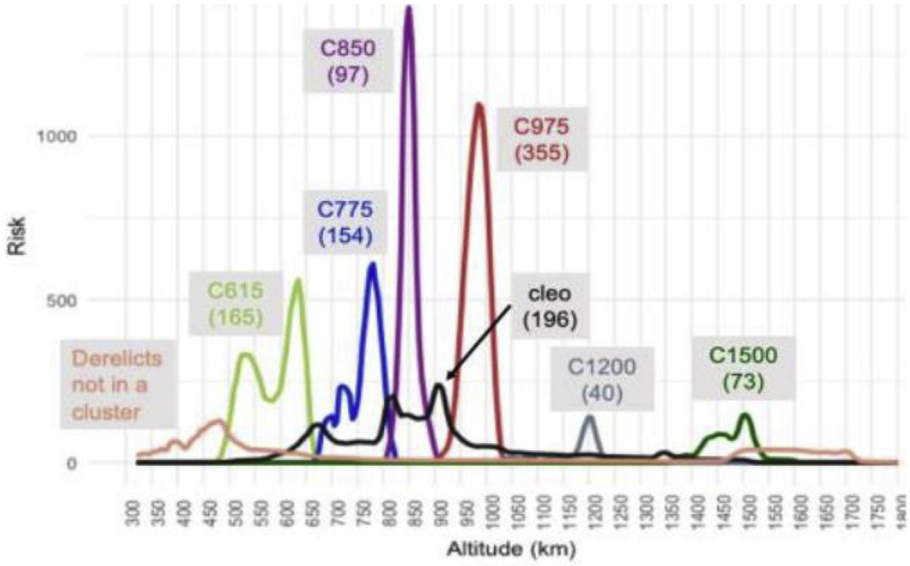

Fig. 2. Debris generating risks – Complete clusters [McKnight R5].

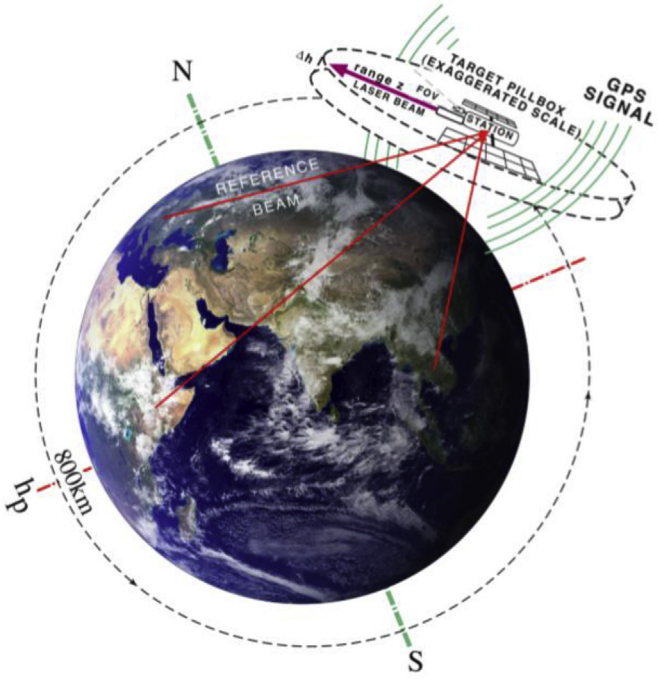

Fig. 3. Orbital laser station Phipps [11].

at shorter range. Periodically, the station's absolute position is determined to by 3 Earth-based stations “pinging” a retroreflector on the station with 100ps pulses simultaneously. The station is also equipped with GPS to assist in the position determination procedure. In this way, the orbit of every satellite it is able to study is determined absolutely with respect to Earth coordinates with at least 10 cm accuracy (see Fig. 4).

The station will use a 5 m focal length, 50 cm diameter optic feeding a 1.5Gpixel gateable array of 2.5 μm pixels with 85% photoelectric efficiency in the visible to establish tracks in sunlight. Its field of view is narrow, 1°. In staring mode, it will permit tracking objects with solar illumination down to 15 cm in size at 1000 km range, and 1 cm at 250 km.

Having established a track, the electro-optical system then does active rather than passive tracking on a selected object using a 50 mJ, 100ps, 1.06 μm, 50 Hz, 2.5 W repetitive-pulse laser. N such data points per satellite encounter with m encounters over several days improves accuracy further and permits orbit determination. At 1,000 km range, only 32 μJ/cm^2 is incident on targets, a fluence level that cannot cause damage to any materials unless further focused. This fluence can be maintained at shorter range by turning down the laser. Range gating together with a 50 nm narrowband optical filter gives adequate signal/background ratios on most targets. Multiple stations are envisioned to increase coverage and data rate.

2.3. Laser and parameters for a single system of the ranging array

One orbiting station can only provide precise location information on a given satellite in one dimension in one interaction, together with more coarse location information on the order of 1 m in the transverse plane. At 50 Hz, we obtain a large number N of data points in one encounter. In m encounters, enough data to determine an orbit for one object is gathered.

The station consists of a laser system and a detection system [11].

The laser system is small and inexpensive (Table 1), so it makes sense to have a swarm of stations in different planes and altitude bands working cooperatively to develop orbits for all objects of interest more rapidly than possible for a single station.

Such a laser exists Off-The-Shelf, (Example: EKSPLA PL2231A) is about $135k [12], but would need to be adapted for orbital operations, mainly on the thermal aspects.

The detection system uses a 5 m focal length, 50 cm diameter mirror together with a 1.54Gpixel array of 2.2 μm detector elements (Table 2) to achieve a 1° field of view. The array is gated to sharply reduce background and increase signal to background ratio.

The station has two operating modes, passive staring solar illuminated target, and active, laser illuminated target. Mirror tilts for ranging laser target illumination. Otherwise, it scans the target plane with a 1° field of view. The telescope shell is 75 cm diameter and 1.25 m long, compatible with half the payload volume of Vega.

In the first (Table 3), the station is normally staring, the laser is off and multiple tracks are created on the array with solar illumination of targets. Parameters employed in the table are based on [12]. In this mode, at 1000 km, a target can cross the field of view in as little as 2.3s.

In Table 3 we show the results of operation on a target with 25% diffuse reflectance into one sterradian, a typical value for aluminum. Note that spectral reflections are ignored in this analysis, and can only

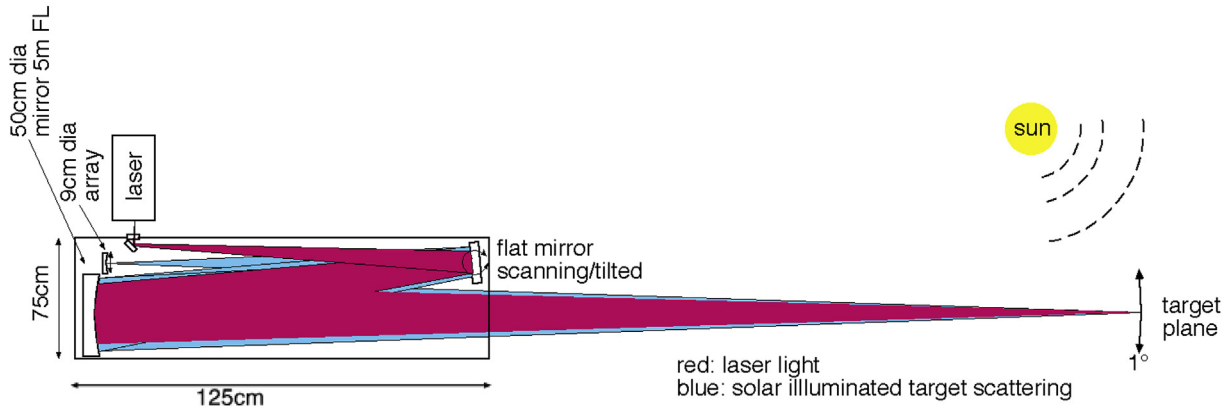

Fig. 4. Two subsystems of the laser ranging system Phipps [11].

Table 1
Ranging Laser Parameters [11].

	Value	Dimensions
Wavelength	532	nm
Pulse energy	50	mJ
Pulse duration	100	ps
Repetition rate	50	Hz
Laser optical power	2.5	W
Laser beam quality M^2	2	–

Table 2
Detection System Parameters [11].

	Value	Dimensions
Center wavelength	550	nm
Optic diameter	50	cm
Focal length	5	m
Field of view	1	deg
Field of view	17	mrad
N pixels	1.54E9	–
Pixel size	2.23	μm
Array diameter (concave)	8.7	cm
Detector electric efficiency	85	%
Dark current at 20 °C [7]	0.4	e/pixel/ms
Design use range	1000	km
Spot size at range	45	cm
Optical filter bandwidth	100	nm
Gate and refresh time	6.7	ms

Table 3
Predicted operating parameters: Passive, staring, sun-illuminated [11].

	Value	Dimensions
Range to target	1000	km
Target diffuse reflectivity R_λ	25	% per sterradian
Assumed range z	1000	km
Assumed target size	45	cm
Sun spectral brightness on target I_λ	1000	W/(m^2sterrad-μm)
Background spectral brightness*	1E-6	W/(m^2sterrad-μm)
Bandwidth	1	μm
Signal S	6.2	pW
Background B	25	zW
Signal/Background	2.5E8	–
Maximum target transverse velocity at range	7500	m/s
Minimum target transit time per pixel	59	μs
Photoelectron number N_{pe}	866	–
Corresponding signal stability 1/SQRT(N_{pe})	3.4	%
Minimum size target that can be seen at 1000 km	15	cm
Minimum size target that can be seen at 250 km	1	cm

*in LEO above 300 km, sun behind us, not looking down at Earth

give better results than diffuse reflections.

Then, the laser is activated and a particular target tracked (Figs. 5 and 6, Table 4). In both tables, “stability” refers to the stability (shot noise) of the return signal, which we take to be unacceptable at Npe = 100 (10%). We see that the signal is easily large enough to overwhelm electrical “shot” noise in the detector.

2.4. Orbital laser ranging station - synthesis

The system described here would allow a gain of two orders of magnitude at least in the accuracy of the orbital debris ephemerids, enabling to lower significantly the rate of false alarms for Collision Avoidance, and enabling JCA type of operations.

We imagine a stepped approach.

The first step would be the development of a small orbital laser ranging system for demonstration purpose. It will only target large known French debris such as old Ariane 1-4 upper stages or observation satellites in order to cope with any potential legal restrictions, and the results of the experiments would be compared to the well-known ephemerids established by the French SST system COSMOS based on the radar Graves.

Once this proof of feasibility is achieved, a first laser ranging station could be developed. It is compatible in size and mass with a dual launch with the European Vega launcher, thus minimizing the overall costs and would be launched in a Sun-Synchronous orbit. The laser station would start collecting information on cataloged debris, assuming a global legal agreement would be achieved in order to allow such kind of operations; the gains coming from such operations should be such that it surely will be considered as general interest, therefore allowable. Only cataloged objects recognized as derelict would be considered; as we would use an initial pointing coming from known ephemerids, the risk of wrongly pinging an active satellite would be very remote. This station would gather a very large number of information, continuously, and the treatment of such big data on ground has to be studied. Depending on the effective performances, it could be useful to have more than one station.

3. Just-in-time collision avoidance (JCA) using orbital laser

3.1. General principle of JCA

The principle of JCA is to impart a small ΔV to one of the two objects, aiming at slightly changing its orbit, semi-major axis and period; when this slight orbital change is propagated in time, it results in a progressive increase of the miss distance at the location of the conjunction. The higher the ΔV, and the higher the propagation time, the larger the miss distance becomes.

For instance, according to Clohessy-Wiltshire Equations of Relative

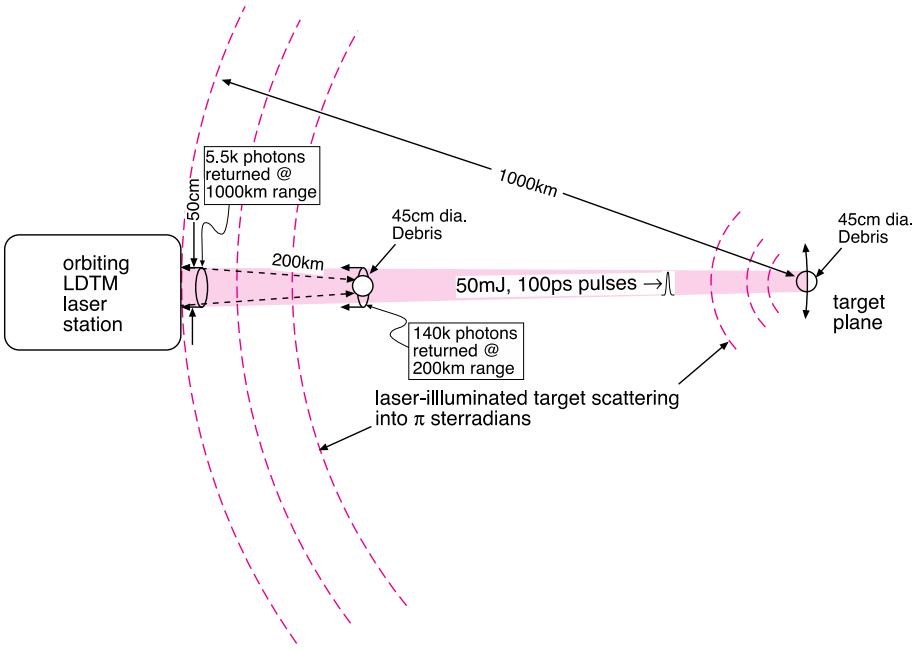

Fig. 5. Active target illumination with 50 mJ laser focused on the 45 cm target returns 5.5k photons at 1000 km, and 140k photons at 200 km [Phipps].

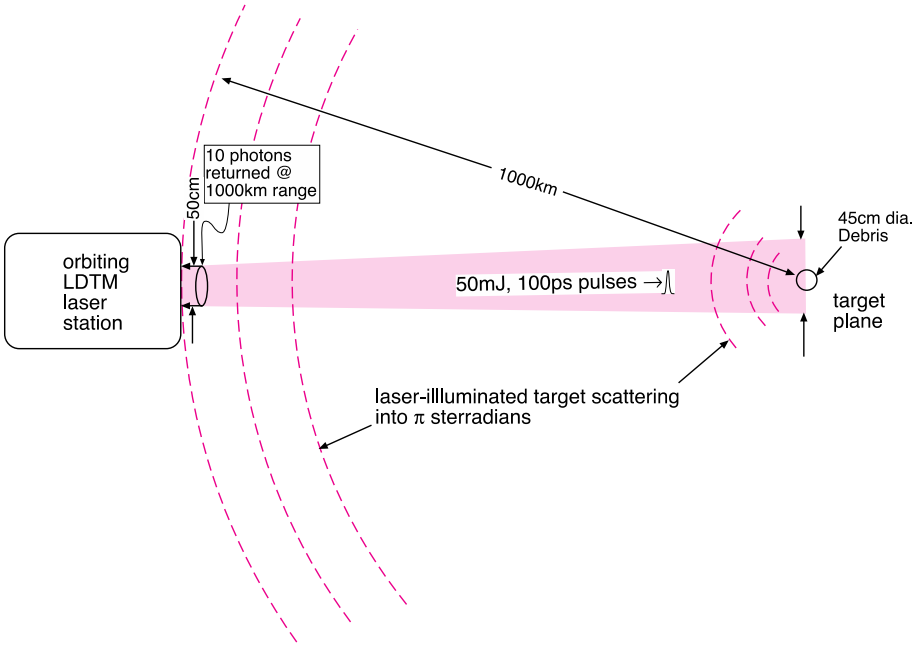

Fig. 6. Active target illumination with 50 mJ beam defocused in search mode to a 10 m diameter at the 45 cm target returns 10photons at 1000 km. This is a minimum for reliable detection. [Phipps].

Motion, imparting a $\Delta V = 3.5$ mm/s along the velocity vector, positive or negative, induces a miss distance increase of 1 km over 24 h. Such effect is globally linear, so $\Delta V = 1$ cm/s 12 h before conjunction would generate a miss distance of 1.5 km.

Concerning the dimensioning of the system, it can be noted that 80% of the collisions imply an object lighter than 100 kg and 95% lighter than 1ton, as was shown by Krag in Ref. [10]; this gives the possibility in most of the cases to choose the smallest debris as the target.

One fundamental hypothesis has to be made here, without which no JCA system could work: it is assumed that the accuracy of the ephemerids of the objects is much better than observed today, typically by one or two orders of magnitude. The system described in the previous chapter, or any as efficient as this one, has to be active at the time JCA operations begin.

Various solutions have been proposed and are currently under study; to quote only a few in a non-exhaustive way:

- Laser-based momentum transfer, from laser ground stations, coupled to laser ranging, would impart the ΔV thanks to light pressure as studied by Krag [10],
- An orbital cloud of tungsten dust was proposed by Sarver, quoted by Levit [13], with the global aim of “cleaning” a complete orbital region from small debris,
- A vapor cloud, kind of “space airbag”, launched on a suborbital trajectory thanks to a sounding rocket, has been studied by Darren

Table 4
Predicted operating parameters: Active, tracking, gated, filtered, laser-illuminated [11].

	Value	Dimensions
Range to target	1000	km
Target diffuse reflectivity R_λ	25	% per sterradian
Assumed range z	1000	km
Assumed target size	45	cm
Optic diameter	50	cm
Optic focal length	5	m
Laser spectral brightness on target I_λ	320	GW/(m^2sterrad-μm)
Background spectral brightness*	1.0	μW/(m^2sterrad-μm)
Gate time = 2z/c	6.7	ms
Bandwidth limited by filter	100	nm
Signal	20	μW
Background	25	zW
Signal/Background	8.0E14	–
Signal energy W_S	2.0E-15	J
Background energy W_B	1.7E-24	J
Signal to background energy ratio W_S/W_B	1.2E9	–
Photoelectron number N_{pe}	4680	–
Target R_λ for N_{pe} = 100 at range z	0.005	% per sterradian
Target size for N_{pe} = 100 at range z	6.9	cm
Signal stability (shot noise) 1/SQRT(N_{pe})	1.5	%

Mc Knight [14],

- A laser station in orbit could slightly nudge the orbit of a debris, considering lasers with very short pulses, very high fluence, vaporizing locally the surface of the debris, generating a recoil effect. Details of such solutions have been extensively presented by Phipps, Bonnal et al. and are not recalled here [15].

3.2. Large Debris Traffic Management (LDTM) using orbital laser stations

An extension of the principle of JCA using lasers, is what we call LDTM.

We showed in Ref. [16] that a single pulsed laser station in a slightly elliptical sun synchronous orbit and oriented 6–18H to always face the sun, at a mean altitude of 900 km with a 1.8 kW average power capability can cause a 4-ton object to miss a collision by 1 km, given 2 days' advance warning.

We propose to continuously manage the position of large hazardous derelicts in orbit, using pulsed laser bursts to slightly nudge the ones which become potentially critical, early enough to keep the required energy at a low level.

The general principle of LDTM is to "correct" the trajectory of any potentially hazardous debris before facing a real risk.

Fig. 7 is a general principle scheme: typical figures could be that any collision risk higher than 10^{-2} would require immediate action; we would correct the trajectory of any debris as soon as its risk would become larger than 10^{-3}, such action aiming at reducing the collision probability to less than 10^{-4} (figures may not be realistic, but mentioned only for the sake of the general principle); the shepherd dogs brings back the sheep close to the canyon as soon as the probability of falling into it becomes larger than 10^{-3}, and does not wait until the last moment to do so.

A continuous monitoring of the LEO population in the critical orbital zones, thanks to the laser ranging system described previously, would aim at providing continuous correction for any debris presenting risk within 2 days.

We used the analogy of "sheep" to be herded, and estimated that there are about 1230 "sheep" at this time, which need nudging at about one per day [16].

We found the change in the period of a target with mass M from illuminating it in-plane with laser power P and coupling coefficient Cm is given by Eq. (1).

$$\Delta T = \pm 12\pi P C_m \tau \left(\frac{a^2}{M\mu}\right) \quad (1)$$

In Eq. (1), μ is the Earth's gravitation constant and a is the semi major axis of the target orbit.

When the ranging system we propose has reduced the position uncertainty to the order of 10 cm, Table 5 shows how significantly low the parameters of a LDTM nudging station can be. Because position uncertainties have been reduced by a factor of 100 relative to today's situation, we could propose a miss distance as low as 10 m. However, we decided to be very conservative, with 100 m miss distance.

Also, we apply the laser pulses one week ahead of an impending conjunction, rather than just 2 days, and use a more realistic example of a 1-ton debris target rather than 4 tons.

In Table 5, we take 10 m miss distance as being a safe value given the new precision with which debris orbits are known. The correction we apply is followed in real-time, closed loop, to avoid unintended outcomes. Design parameters are based on [17–19].

3.3. Synthesis on laser nudging and LDTM

Following the two first development steps described in §2.4, a third step corresponds to the development of a slightly larger station than the simple ranging one enabling small orbital changes to potentially hazardous debris; this Large Debris Traffic Management (LDTM) system will be coupled with the laser ranging function in order to minimize the rate of false alarms. Thanks to the increased precision of ephemerids, the requirement in terms of pulse energy remains low.

The ultimate step would be the use of such systems to modify significantly the orbit of large derelicts, such as old GEO satellites, as previously proposed in the L'ADROIT descriptions [12].

4. Just-in-time collision avoidance (JCA) using cloud of particles

Inserting a cloud of gas, dust, particles in front of one of the two objects will induce a drag, i.e. a trajectory modification which can generate a miss distance high enough to avoid a statistically possible collision.

A very general schematic of the idea is given by Fig. 8 from McKnight.

The authors have been studying a solution considering the launch on a suborbital trajectory of a cloud of small particles, generating some drag on the debris when it crosses it. Following the first evaluations [21], 3 feasibility points were raised and treated during a dedicated study performed by CT-Ingénierie-France and CNES since mid-2018, relative to efficiency of the system, phasing of the operations, and design of the particles ejector.

4.1. Efficiency of the JCA system using a cloud of particles

Considering the 3 main clusters of large derelict objects mentioned in §1, we considered that the debris could be in any orbit between 600 and 1200 km, any inclination; we did not consider the slight eccentricity of the real orbits, as this is easily computable and does not represent any hurdle. We considered a maximal debris mass of 2000 kg; it means that when an SL-16 is associated to a collision, we would nudge the other debris, statistically much lighter than 1ton. The 2 tons' requirement covers any collision implying an SL-8 stage.

Typical operations would be based on the initial identification of a potential collision above the admissible thresholds, 36–72 h before the computed near conjunction. This would leave some time to refine the trajectory of the two objects, reducing the dispersions on ephemerids, and consolidating the probability of the collision risk. The time between the beginning of the launch operations and the application of the braking ΔV is considered to be less than 24–48 h; it includes the time to prepare the rocket and the phasing delay linked to be at the nominal

Fig. 7. General principle of LDTM [Initial image © Juliette Samson, Amaryllis].

Table 5
LDTM system parameters [11].

	Value	Dimensions
Pulse energy W (2 pulses per burst)	480	J
Wavelength	532	nm
Pulse duration	100	ps
Long term laser average power in 2 days	1.5	mW
Assumed target C_m	30E-6	N/W
Optic diameter	2	m
Laser range z	400	km
Assumed target mass	1000	kg
Applied Δv during burst	29	μm/s
Resulting miss distance	1.1	m/orbit
Miss distance in 7 days	100	m

conditions for the launch. The requirement is to launch 12 h latest before the foreseen conjunction.

The specification for the relative positioning of the particle generator and the debris is that the distance d when expelling the particles shall be less than 1 km, and the safety margin, difference between the culmination altitude of the braking system and debris orbital altitude precision shall be larger than 500 m (value which can be refined once realistic accuracy of the system is determined).

The efficiency of the system as a function of the angle of the jet with respect to the orbital path has been established, and is not strongly modified between 30 and 90°. The out-of-plane trajectory of the JCA system (z on Fig. 9) can be compensated by the proper tilting of the ejector to make sure it aims at the trajectory of the debris.

An example of the effect of the braking on the debris is shown in Fig. 10. This simulation shows the result of a braking of $\Delta V = 7.7$ mm/s propagated during 12 h on a 1200 km circular orbit debris. Fig. 10 shows the new debris trajectory in a reference frame fixed to the initial debris trajectory. The reference frame is the LVLH (Local Vertical Local Horizontal) relative to the initial debris trajectory, i. e. without braking, with the axis shown as Vbar for the velocity direction (i.e. local horizontal) and Rbar for the direction from earth to the debris (i.e. local vertical). It allows seeing the effect of the braking on the debris, compared to a fictive debris which has not been decelerated.

After n = 7 revolutions, i.e. almost 12 h, the new debris trajectory is almost 1000 m away from its initial trajectory. The avoidance distance thus depends on n, the number of revolutions the braking effect can be propagated on but also on ΔV, the deceleration transmitted to the debris. The Clohessy-Wiltshire Equations give the following formula for period difference ΔT induced by a deceleration of ΔV:

$$\Delta \mathrm{T} = -3.\ T.\ \Delta V/\mathrm{V} \tag{2}$$

Leading to the avoidance distance δL:

$$\Delta L = -3.\ \mathrm{n}.\ T.\ \Delta V \tag{3}$$

This calculation can be coupled with the debris mass and friction coefficient (included in ΔV calculation) to compute the required mass of particles hitting the debris, called effective mass. This is shown in Fig. 11 for a 1500 kg, 800 km altitude debris with a friction coefficient of 1.7. The graph shows the required effective mass depending on the avoidance distance, for 6 and 12 h of propagation of the braking effect.

As a result, the necessary effective mass required to perform the mission is surprisingly small. As a typical example, providing a $\Delta V = 7.7$ mm/s to a 1.4 tons debris requires only 3 g particles; applied 12 h before the closest conjunction, it would increase the miss distance by 1 km. The main difficulty is to locate the particles cloud close enough to the target to guarantee that at least 3 g of particles impact it!

It can be noted here that such approach remains very conservative, as we don't consider here the braking effect of the plasma ejection resulting from the collision with the particles.

4.2. Phasing of the operations

One fundamental challenge of the operation is to guarantee the proper phasing of the suborbital rocket trajectory and the passage of the debris to be deflected. If, for instance, you would have only one launch base and a purely vertical launch capability only, the probability to have the debris passing precisely at the proper time and proper location would be very small.

The first studies led to disregard solutions based on sounding rockets launched from ground bases, too limited in performance in general, with limited lateral deport in particular, and not optimally located. The reference solution here considers airborne suborbital rocket, enabling some cruise and adjustment to the optimal geographical location prior to the launch.

In order to reach any orbit, a certain number of ground bases from which the carrying planes can takeoff are required. This number depends on:

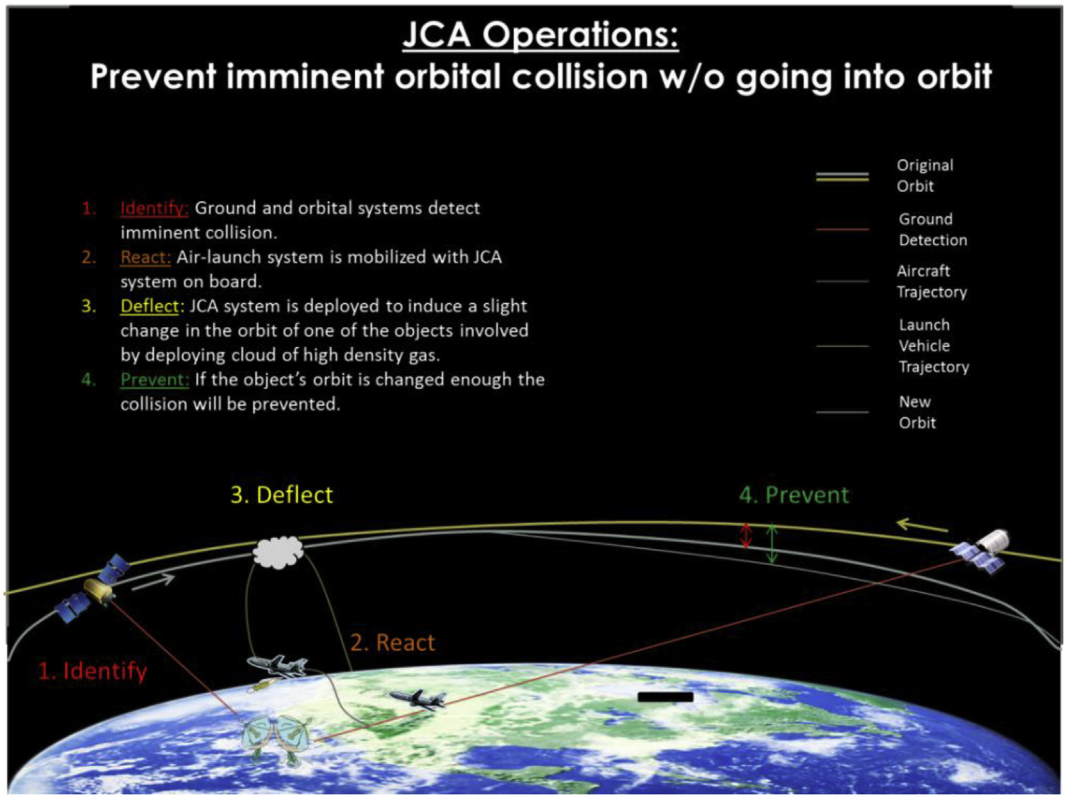

Fig. 8. Just-in-time Collision Avoidance – General principle. Note that this artist's depiction shows the collision being avoided very near the "deflect" stage but in reality the derelict will be nudged at least half of an orbit before the predicted collision [20].

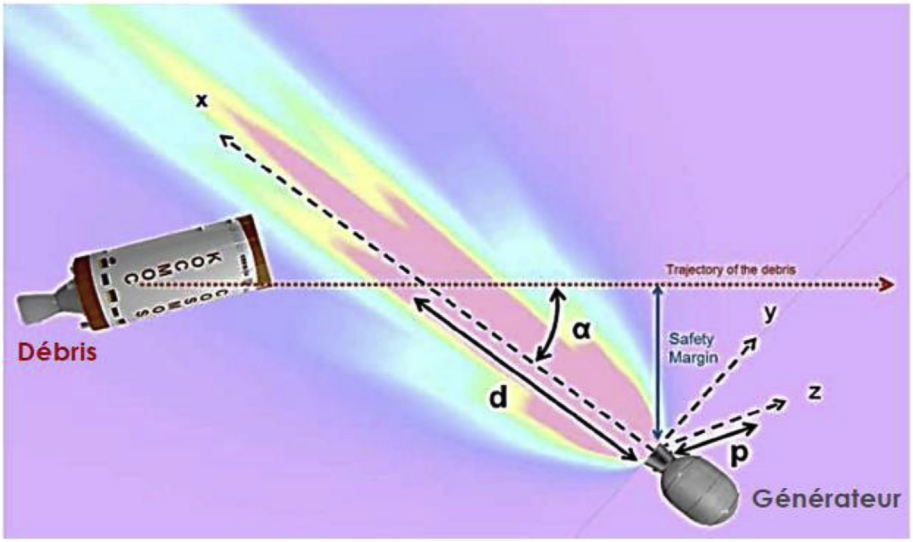

Fig. 9. Relative positioning of debris track and JCA system Dupont & al., [22].

- The capability of lateral "out-plane" shift by the system, both the plane and the rocket,
- The delay between the decision to engage the procedure and the expected collision. Fig. 12 shows the timeline of the process: the acting time TA is the time between the decision to engage DE and the moment when it is too late to act on the debris DF. One of the requirements is that the acting time shall be small enough to cope with the precision of the debris positions prediction (TP = 24 h) and the braking propagation time required (TB = 12 h).
- The time TA is used to wait for a suitable debris pass and to launch, catch-up with the lateral deport and reach the apogee where the systems acts on the debris. Its maximum value is 12 h but the baseline for the study is 6 h

We considered bases located near the equator in order to be able to reach any orbit inclination; obviously, solutions with slightly higher latitudes would work as fine, considering the cruise range of the carrying plane. Moreover, one of the drivers of this analysis is the orbital drift, and due to the equatorial constraint, the equatorial drift. Fig. 13 shows the worst case in the range of orbit studied for this analysis (maximal altitude 1200 km and polar inclination 90°): up to 3060 km can separate two orbits at the equator. This number was used as

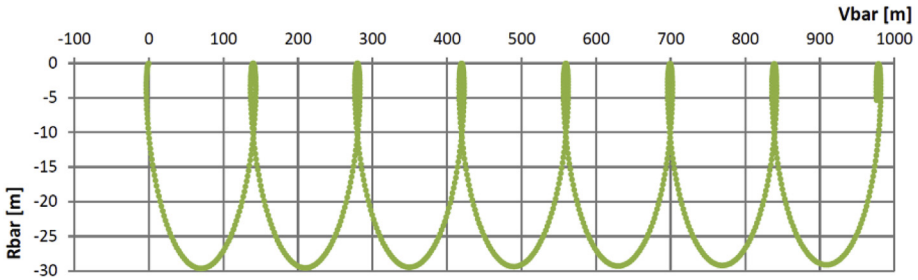

Fig. 10. Debris trajectory after braking in the LVLH frame fixed to the trajectory before braking. Braking of 7.7 mm/s, simulation duration 12 h Dupont & al., [22].

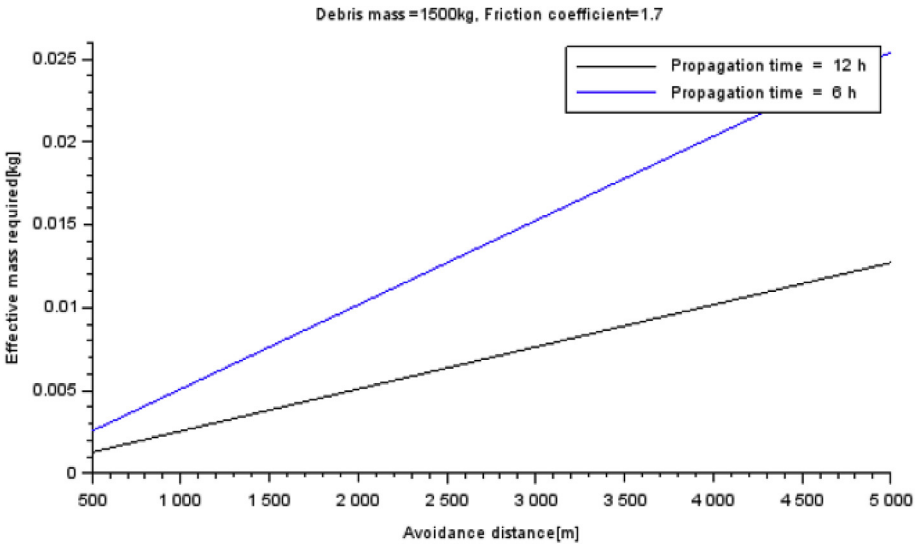

Fig. 11. Effective mass required for avoidance distance and propagation duration Dupont & al., [22].

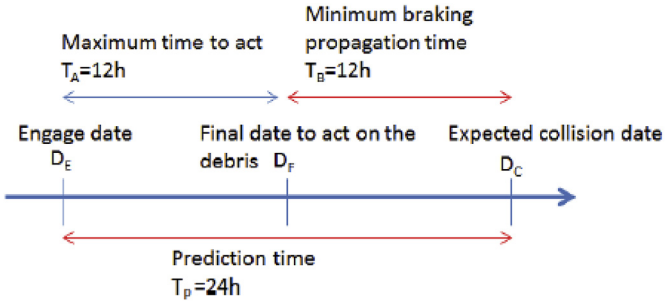

Fig. 12. Operations timeline Dupont & al., [22].

Fig. 13. Maximal orbital drift Dupont & al., [22].

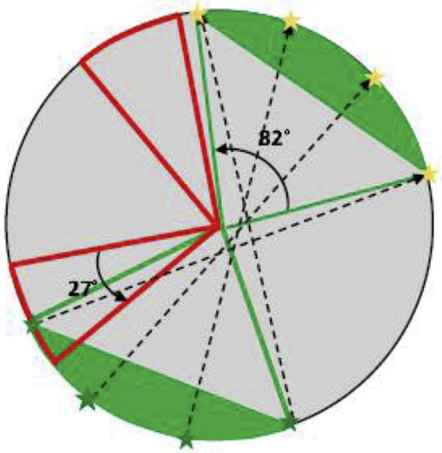

Fig. 14. Ground bases locations Dupont & al., [22].

requirement for the plane.

A geometrical approach can be used to compute the number and locations of the ground bases. Fig. 14 shows in dashed line the orbit of the debris during 6 h in a fixed Earth reference: the ascending and descending nodes will be shifted by 82° in longitude in 3 periods (5h30), the equivalent of 3 × 3060 km around the equator. The green zone shows the equatorial footprint for both nodes. One possible solution of coverage by the ground station is shown by the two red triangles. They represent the necessary coverage zone (at the equator): if both coverage zones are 27.3° large in longitude and 90° one from the other, at least one dashed line will always fall into one of the triangle.

Table 6
Number of bases required Dupont & al. [22]

Acting time	Range (km)	Total number of bases required	Number of coverage zones required
6h	3060	1 + 1	2
	1530	1 + 1	2
	765	2 + 2	2
	383	4 + 4	2
	191	8 + 8	2
	96	16 + 16	2
12h	3060	1	1
	1530	1	1
	765	2	1
	383	4	1
	191	8	1
	96	16	1

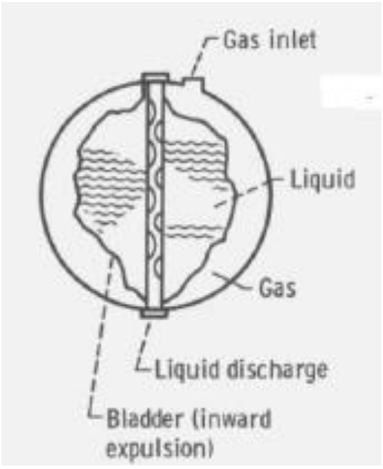

Fig. 15. Schematic of a spherical bladder tank [R23].

Fig. 16. Ariane 5 58 L hydrazine bladder tank ArianeGroup [24].

This shows that at least one opportunity for reaching the orbit occurs in 6 h. If the triangles are smaller or with a different angular separation, this is not ensured anymore.

The number of bases required in this coverage zones can be computed using the apogee range of the system. Indeed, the 27.3° longitude represents 3060 km on the equator. The number of bases per triangle is 3060 km divided by the range of the carrying plane and launcher. Table 6 shows the number of coverage zones and the number of bases required for a given acting time and a given launcher range.

Fig. 17. GOLauncher-2 [GenerationOrbit.com].

This table shows a worst case of 32 bases, for a worst case of a range lower than 100 km and an acting time limited to 6 h; this would simply be too expensive and complex to manage and keep operational 24/7. On the opposite, considering an acting time of 12 h with a 1000 km range for the plane would necessitate 2 departing bases at the most. This explains the need for a large range or a large acting time in order to reduce the number of bases. With the air launched system considered as reference here, the range will be done by the carrying plane. Improvement of the Space Situation Awareness and the accuracy of the observations and ephemerides of the space debris will also tend to increase the acting time.

It is also important to mention the redundancy of the bases. Indeed, if for a meteorological reason, one of the bases is unable to perform the required launch, another base shall be able to replace it and perform the launch. This particular problem is very global and has not been addressed in this study but will impose extra bases to the system.

4.3. Particle ejection

The initial simulations performed on the system [21] were based on a cloud of combustion gases coming from a Solid Rocket engine. The conclusion of that study was that solid particles impact would be much more efficient, and that the ejection velocity should be as low as possible in order to avoid too much dispersion.

The current study therefore considered as baseline small solid particles. These particles should be of high-density to keep the jet direction and avoid diffusion with gas expansion; they shall have a maximal size of 50–100 μm in order to avoid significant ejecta at collision on the debris, but have a size of 5–10 μm at least to be efficient. We wanted particles to be commercially available off-the-shelf, cheap, with a constant diameter. As an arbitrary choice, we considered an action of the ejector during 10 s, in order to have some built-in robustness. The total mass of particles resulted to be in the range of 10 kg. We selected 50 μm copper marbles, but similar highly dense material could work as well.

A very wide trade-off was performed to find the best concept for the ejector. More than 12 potential solutions and variants were identified, and the selection was done following a Model-Based System Engineering (MBSE) approach set in place by CT Paris, considering as major criteria the global mass, the reliability of the complete function, the dispersion of the particles cloud both in time and in space, and the availability of the solution, TRL and Cost.

The preferred solution turned out to be a classical bladder tank, such as widely used for propellant tanks on satellites and launcher stages. The principle is described in Fig. 15, from Ref. [23]: the tank is composed of an external metallic shell and houses an internal polymer bladder which crushes around a stand-pipe with holes. The volume between the external shell and the bladder is pressurized using a neutral nontoxic gas, and the volume inside the bladder contains the fluid which has to be ejected. The stand-pipe enables the expulsion of the fluid through the tank liquid discharge orifice which include a pressure

Table 7
Typical dimensioning of the suborbital rocket.

Stage	Inert Mass [kg]	Propellant mass [kg]	Combustion time [s]	Vacuum ISP [s]	Nozzle exit area [m^2]
1st Stage	241	1615	27	300	1
2nd Stage	80	538	13	300	0.6
RDV (inc. generator)	241				
Fairing	50				

Fig. 18. General layout of the of the suborbital rocket.

Table 8
Flight scenario sequence.

Time (s)	Event	Altitude (km)	Flight Path angle (°)
0	Rocket drop	12	20
5	1st stage ignition	12.2	4.1
32	1st stage end of burn 28.4s coasting phase, 1st stage separation	33.2	76.6
60.4	2nd stage ignition	86.9	74.9
71.1	Fairing jettisoning	113.8	84.1
73.4	2nd stage end of burn 540.6s nominal ballistic phase to apogee, terminal stage guidance	122.4	85.0
614.1	Nominal apogee	1200	0

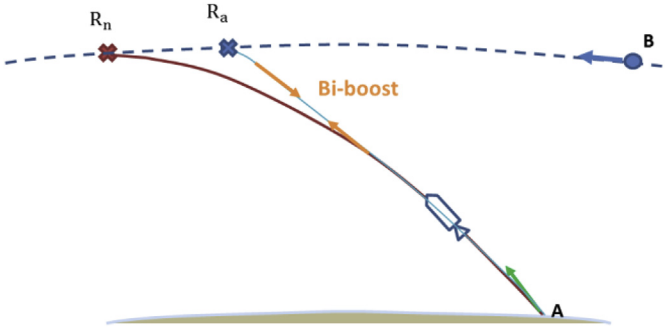

Fig. 19. Typical maneuver to compensate a delay in launch time.

regulator (if necessary) and a nozzle (not shown on the sketch).

We selected one well-known tank, used on Ariane 5 but also on the ARD reentry demonstrator flown in 1998, pictured in Fig. 16 from Ref. [24]; it is manufactured by ArianeGroup and is an off-the-shelf product.

This tank, 48 cm in external diameter, has a total volume of 58 L and an internal volume under the bladder of 39 L. The external shell is made of Titanium Ti6AlV and the bladder is made of Ethylene-Propylene-Dyene monomer. The Maximal Expected Operational Pressure (MEOP) is 26 bars, and the Burst Pressure is 52 bars. We would use dry air or Nitrogen for pressurization.

The fluid shall have a high viscosity in order to guarantee the dispersion of the particles in the fluid stable in time with no sedimentation

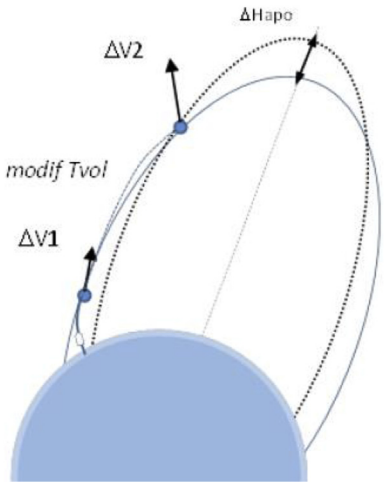

Fig. 20. Typical maneuver to compensate a modification of target location Dupont & al., [22].

during storage or under the acceleration forces of the flight. Calculations were performed for a variety of fluids to determine what the maximal migration velocity U_{tc} would be following Eq. (3), for a particle of diameter d and density ρ_s, under an acceleration g, migrating in fluid with density ρ_L and dynamic viscosity μ.

$$U_{tc} = \frac{d^2.\ g}{18.\ \mu}.\ (\rho_s - \rho_L) \tag{4}$$

This principle was evaluated for d = 50 μm copper particles with an acceleration of g = 50 m/s^2, which is by far the worst condition that would occur in the life of the system, as if the maximal trajectory acceleration was applied constantly. Application of this principle to water, oil SAE10W and glycerin, shows migration velocities respectively of 5.6 cm/s, 0.56 mm/s and 36 μm/s; in this last case, with glycerin, the particles would not migrate at all and remain well dispersed within the fluid.

The tank itself, bladder and stand-pipe included, has a total mass of 8.5 kg. We consider an additional dry mass of 6.5 kg to take into account regulator, valves, throat, nozzle … We would load the tank with 17 kg particles, 33 kg glycerin, 700 g pressurized Nitrogen, leading to a total mass for the ejector system equal to 65 kg.

4.4. JCA system architecture

Numerous air-borne launcher have been studied since decades, so the performances of such systems are well known. A bibliographic study was performed considering a 2.8 tons' sub-orbital rocket, 7 m long and 90 cm in diameter (values are justified later in the paper). Considering business jet, fighter aircraft, commercial aircraft and dedicated planes, the final choice was to baseline business jets such as Dassault Aviation Falcon 7X or Gulfstream IV. The Falcon 7X for instance would have a published range of 8,800 km with the rocket defined above, carried under its fuselage. Performances are very similar for the Gulfstream, as presented for instance in the GOLauncher-2 from Generation Orbit, Fig. 17.

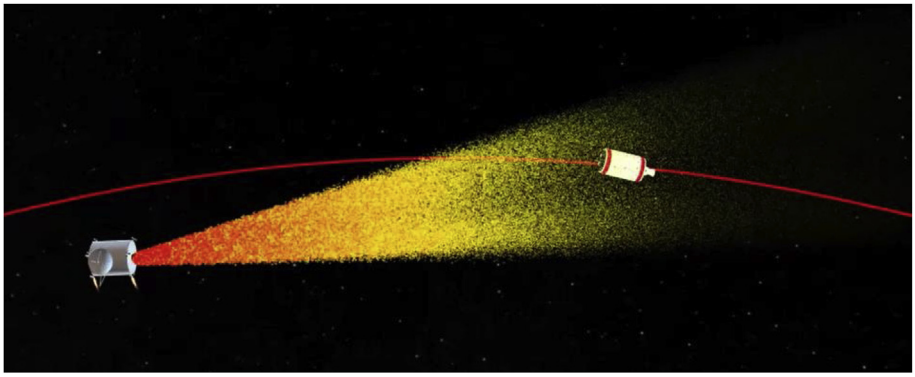

Fig. 21. Artist view of the system during particle ejection phase Dupont & al., [22].

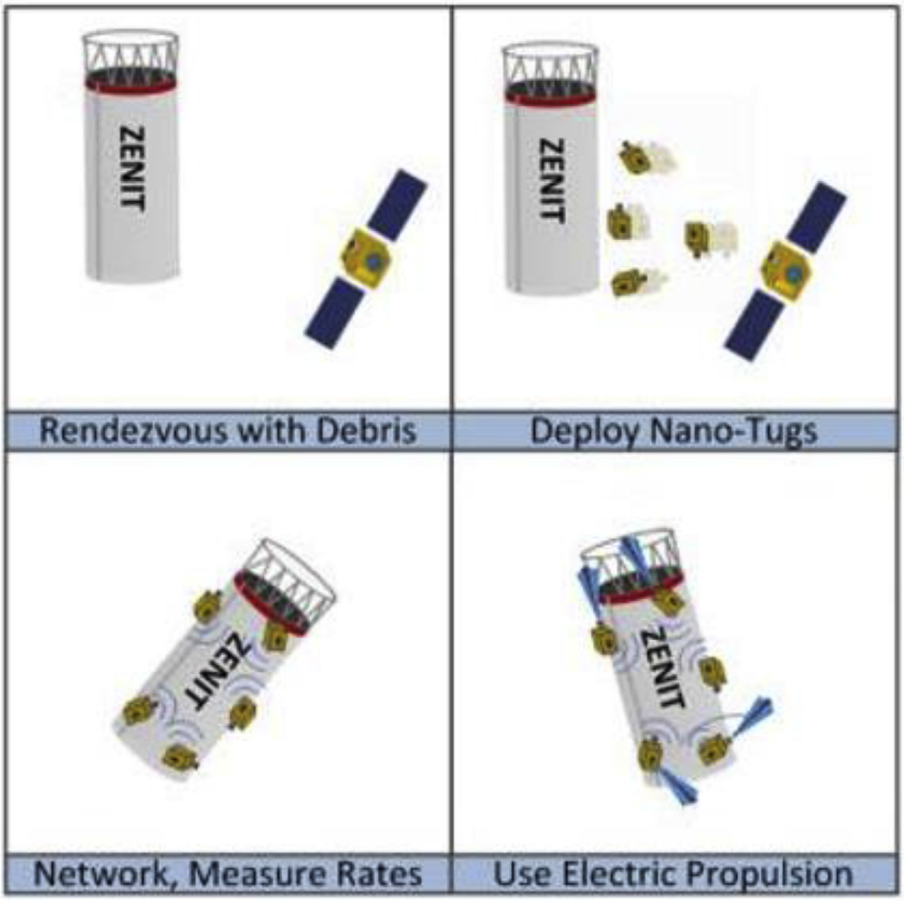

Fig. 22. General principle and function of Nano-tugs McKnight, Santoni [25].

The preliminary concept for the sub-orbital rocket is a three stages vehicle:

- The first stage performs the atmospheric phase, from the separation with the plane to the edge of atmosphere, with a guidance law based on incidence; its propulsion is based on storable non-toxic liquid propellants such as H_2O_2-Kerosene,
- The second stage provides most of the ΔV and enables to reach the target point for the separation with the 3rd stage performing a dog-leg if necessary to reach the proper azimuth. It uses the same kind of propulsion as the 1st stage and includes the performance reserve required to compensate the scattering in hardware definition, as well as atmospheric dispersions,
- The 3rd stage aims at performing the final approach and rendezvous, and the proper orientation of the particles ejector; it is 3-axis controlled and potentially uses a monopropellant system.

The general dimensions of the rocket have been chosen in a reverse way to fit exactly the maximal performance allowable for the Falcon 7X: 7 m overall length, 86 cm in diameter (under fuselage) and a maximal mass at plane take-off of 2.8 tons. Table 7 presents more details on the general architecture (Fig. 18).

The corresponding flight sequence is described in Table 8.

An important point which acted as a driver for the sizing of the launcher is the general robustness to all the dispersions which can be encountered. Some parameters can reasonably be considered as known with a very high accuracy, such as the position of the orbital plane of the debris; the position of the debris on that trajectory should be well

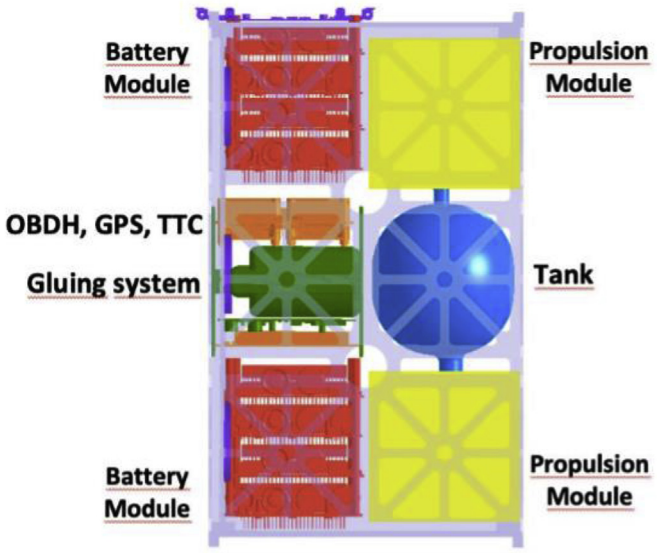

Fig. 23. Schematic configuration of internal components in a nano-tug McKnight, Santoni [25].

known also: a typical uncertainty of 1 km on the position corresponds to ± 130 ms in time, and the preliminary requirement for the system was to have an ejection of particles lasting 10 s, so there should be plenty of margin.

But the initial position of the airplane may be non-optimal, in case of meteorological problem in the launch zone, inducing some variations in position and in time of launch. The system shall be capable to perform a time correction such as schematized in Fig. 19; a bi-boost strategy has been defined and detailed for the case where the launch from point A was not at the optimal time, for which debris B would have been in point Rn nominally, reaching the Ra real case slightly later. In a similar way, the system shall be capable to modify the flight trajectory and mission duration to reach any point in 3D in the vicinity of the planned target; Fig. 20 schematizes this kind of Lambert optimal trajectory to modify the target during flight. Significant ΔV margins have been considered to take into account this requirement for robustness.

4.5. Synthesis on the JCA system based on particle cloud ejection

The initial study performed on the idea of using a cloud of particles to slightly nudge the trajectory of a large debris pointed out 3 feasibility points which had to be studies further.

First, the global efficiency of the particle cloud has been consolidated, showing that indeed only a tiny fraction of the particles have to impact the debris to impart the required braking ΔV: the system was dimensioned considering 17 kg particles, when 3 g would normally be enough, if correctly located! The ejector spreads the cloud of particles with a relative velocity of 100 m/s during 10 s, starting 5 s before the theoretical passage of the debris; this way, the cloud spreads over 1 km centered on the nominal targeted point (see Fig. 21).

Second, the phasing between the ascent trajectory of the rocket, precisely its culmination point, and the debris is tricky. The solution selected here considering a modern business jet offers enough payload capacity and a very large range of more than 8,000 km, enabling a couple of planes to reach any point for any orbit up to 1,200 km altitude within a couple of hours.

Third, the ejector system was defined, based on a very well-known bladder tank used on Ariane 5 to expel Hydrazine; the adaptation to a much more viscous fluid with particles dispersed in its bulk has to be verified, but no blocking point is identified so far.

The overall dimensioning of the system, although preliminary, was performed considering robustness at mission and architecture levels to cope with trajectory dispersions, coming from the debris, the plane or the rocket.

The system is potentially recoverable and reusable: to cope with the safety rules imposed by the French Space Operations Act, the operations take place above oceans, which means that simple parachutes and floatation devices may enable recovery of the two fist stages, at least.

The next step consists now in imagining an international cooperative scheme to deploy such system, with 3 or 4 launch bases spread around the world, striving together to avoid THE collision between two very large derelict objects which would strongly question the sustainability of our space operations. Even before that, as said in the introduction, we shall aim at improving drastically the accuracy of the ephemerids of our space objects, otherwise such JCA ideas are not realistic.

5. Nano-Tugs

5.1. General principle of nano-tugs

In order to have a complete picture of the different ways enabling to avoid a deterministic collision between non-maneuverable orbital objects, it may be interesting to mention here the initiative dubbed “Nano-tugs” published by McKnight and Santoni [25].

The general idea is to attach a swarm of nano-satellites on a large potentially hazardous derelict, such as a Cosmos-3M or Zenit upper stage, and to operate them first to determine the attitudes of the object, second to despin it, third to slightly modify its trajectory in case of a predicted collision probability above a given threshold. Nano tugs, schematized in Fig. 22 would be “*bringing derelicts back to life from a collision avoidance and self-awareness perspective*” to quote the authors of [25].

This concept is an evolution of an idea initially proposed by McKnight, DiPentino, Kaczmarek & Knowles in Ref. [26], which aimed basically at detumbling the debris; the recent evolution of this idea includes the use of residual propellant to enabling a small nudging of the hazardous object.

The dimensions of such modules can remain quite small.

In Ref. [25] the authors consider a system with a Xenon based electric propulsion providing 0.7 mN thrust with an Isp of 800s.

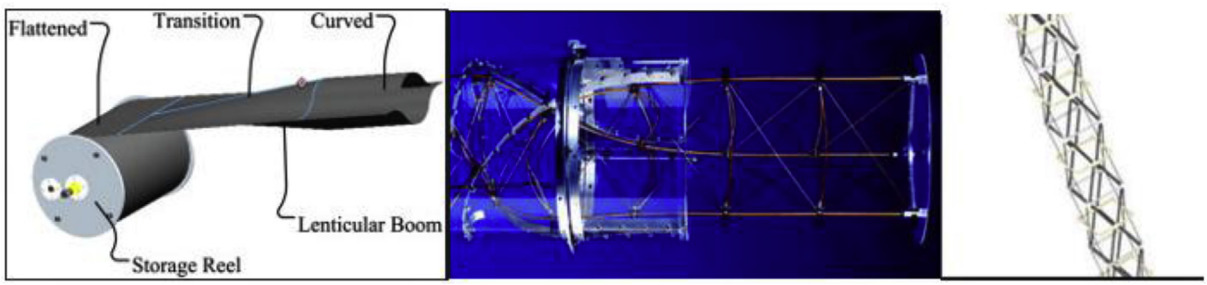

Fig. 24. Deployable interface legs (notional).

Modes of Manipulation

	Pull	Shear	Twist
Sheet Metal	Poor	Exceptional	Exceptional
Painted Metals	Poor	Inconclusive	Inconclusive
Photovoltaics	Poor	Inconclusive	Inconclusive
MLI	Poor	Exceptional	Exceptional
Kapton/Mylar	Poor	Effective	Effective
Wood	Poor	Poor	Poor
Paper	Effective	Effective	Effective

Results of testing using ElectroGrip© 11.5" x 11.5" DR5 Electrostatic chucks
- 2-4kV high Voltage range with 6 poles & 3 phases
- Close Proximity Sensing up to about ½ meter

3-phase gripper performance increases marginally in low moisture @ 1 atm. (from 51% RH vs. 0.1% RH at 68ºF)
Toggling down period of voltage cycling rate from quick to slow induces notable stronger Johnsen-Rahbek attraction effect

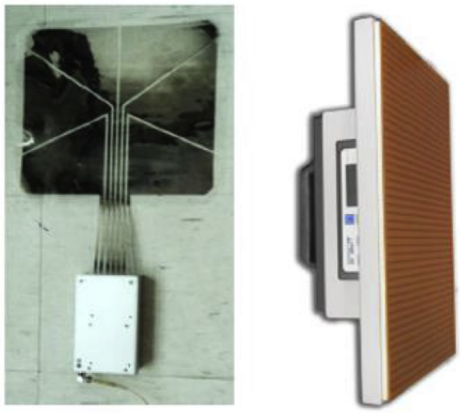

ES\EA grippers by ElectroGrip, Co. and GrabIt, Inc

Fig. 25. Electrostatic gripper ElectroGrip and GrabIt, quoted by Gagliano NASA [28].

Detumbling an SL-8 upper stage from an initial 3°/s spin rate would require 29 g propellant. A collision avoidance by 200 m would then require only 1.5 g! A total operational lifetime of 20 years, assuming 2 maneuvers per month, would then equate to a total propellant mass in the order of 750 g. The corresponding tank would be less than 10 cm in radius, which corresponds to the classical figures considered for Cubesats; the typical design studied by McKnight & Santoni would be a 6U cubesat, schematically depicted in Fig. 23.

5.2. Mosquito

In parallel to this work on nano-tugs, a slightly similar concept is under study at CNES, dubbed the "Mosquito".

It would be a relatively small cubesat, 8–12U, launched in piggyback in an orbit close to one of the large derelicts, with the following functions:

- It would perform a rendezvous with the target object, using an electric propulsion Xenon or Iodine based for the transfer, then cold-gas or dual mode propulsion for the rendezvous itself,
- It would then inspect the target from a small distance, 1 m or so, in order to evaluate the effects of aging on the structures, thermal protections, global integrity, and determine the general attitude motion of the target,
- As a function of the tumbling mode identified, the Mosquito would do a physical contact with the target, the interface being 4 deployable legs, as depicted with the examples from Fig. 24, rolled boom, torsional boom or pantograph,
- The interface force, very low, force could be provided by small electrostatic grippers, such as depicted in Fig. 25; such interfaces are reversible, which means that it is possible to change location on the target; Gecko-paddles type of interfaces can also be considered (single foot of a Gecko could produce 100 N adhesive force [27]),
- The main mission of the Mosquito would be to characterize the impacts thanks to a Macro-camera, but this function is not described here, being subject of another publication
- The propulsion system of the Mosquito could be triggered in order to command a small change of trajectory of the debris, providing effective JCA capability.

Preliminary work on this concept shows that the total ΔV required would be in the range of 500 m/s, by far the largest part of this budget being the required orbital change from the initial orbit to the targeted one (worst case simulations showing a need for 340 m/s for this phase); the close distance rendezvous maneuvers and nudging operations are more than one order of magnitude lower.

Considering, as a notional example, a Busek-BHT-200 Hall Effect Thruster [29] functioning with Iodine (as already demonstrated, but acknowledging potential thermal problems), the amount of propellant would be in the order of 730 g.

The efficiency of the system depends naturally on the proper orientation of the thrust; in order to have a high efficiency, it would be necessary to aim at ± 30° with respect to the velocity vector (87% efficiency).

Considering the 3 "basic" tumbling modes, the "bicycle wheel" (rotation plane equal to orbital plane), "helicopter mode" (rotation plane parallel to Earth surface) and "propeller mode", (rotation plane perpendicular to velocity vector), there is always a location on the debris where the thrust can be efficient, even if intermittent (which is anyhow needed to minimize the size of the solar panels). In the case mentioned above, providing a 3.5 mm/s ΔV to a 1 ton debris (see §3.1), this equates to a total thrust duration of 300s. Considering firing durations of 20s per rotation, the final nudging maneuver would last 1800s, or 1/3 of the orbit. The process can be slightly improved playing on the differential length of the interface legs.

6. Conclusions

A lot of work has been devoted to ADR these last 10-12 years, with numerous good concepts being identified, studied, developed and demonstrated, either on ground, or through 0 g drop tower or plane, and even recently in orbit.

However, when considering the initial requirements established for ADR, for instance by NASA [6], stating that some 5 to 10 objects would have to be removed to stabilize the orbital population in LEO, it may be necessary to revisit slightly this evaluation.

- First, the mitigation standards (with all their variants, codes of conduct, guidelines, charter, law) have not yet shown any efficiency on the evolution of the population of derelict objects in orbit (as an example without any analysis, 698 objects entered the public catalog in 2019, and 321 only were removed from orbit, a net balance

of 377),
- Second, the number of nanosatellites has drastically increased, and most of them are non-maneuverable, but definitely too small to be “valuable” ADR targets,
- Third, the economical scheme of ADR still has to be demonstrated; in that field, ESA is starting a very interesting demonstration with ClearSpace, aiming both at demonstrating technically the feasibility of ADR on a real orbital debris, but also at elaborating an economically viable operational scheme.

ADR is a statistical action in the sense that the debris which are removed are not the ones which statistically would have generated a collision; it is just shown that to prevent one massive collision within the coming 20 years, you need to remove 100 large debris, in addition to coping with a strict 90% compliance to mitigation rules.

In addition to such “strategic” long-term actions, it is fundamental to prepare for detectable, thus avoidable, large collisions among non-maneuverable objects. To that extent, JCA shall be given a good priority as well, in parallel to ADR.

The authors believe that several credible solutions exist and would be worth studying in more depth at international level; as a minimum short term action, priority should be given to the improvement of the accuracy of ephemerids, without which not much efficient operation can be done to preserve the orbital environment.

Acknowledgement

Dominique Mazouni (DMZ, France) contributed in the Working Group dedicated to the ejector solution §4.3.

References

[1] D. McKnight, T. Maclay, Space environment management: a common sense framework for controlling orbital debris risk, Proc. AMOS (2019).
[2] D. Kessler, B.G. Cour-Palais, Collision frequency of artificial satellites: the creation of a debris belt, J. Geophys. Res. 83 (A6) (June 1978).
[3] D. McKnight, S. Behrend, P. Casey, Insights gained from the massive collision monitoring activity, Proceedings of the 9th IAASS Conference, #28A, France, Toulouse, October 2017, p. 512.
[4] D. McKnight, K. Walbert, Proposed series of orbital debris remediation activities, Proceedings of the 7th European Conference on Space Debris, Darmstadt, Germany, April 2017.
[5] D. McKnight, R. Arora, R. Witner, Intact derelict deposition study, #6011, Proceedings of the 1st International Orbital Debris Conference, Houston, December 2019.
[6] J.C. Liou, Modeling the large and small orbital debris populations for environment remediation, #1.1, Proceedings of the 3rd Workshop on Modeling and Remediation, Paris, France, June 2014.
[7] D. McKnight, F. Di Pentino, K. Walbert, S. Douglass, Developing a tactical adjunct to ADR to insure a sustainable space environment, IAC-15-A6.2.7, 65th International Astronautical Congress, Jerusalem, Israel, October 2015.
[8] D. McKnight, Engineering and operational issues related to just-in-time collision avoidance (JCA), Proceedings of the 6th EUCASS Conference, Krakow, Poland, July 2015.
[9] G.E. Peterson, M.E. Sorge, J.P. McVey, S. Gegenheimer, G.A. Henninge, Tracking Requirements in LEO for Space Traffic Management in the Presence of Proposed Small Satellite Constellations, IAC.18.A6-7.6, (October 2018) Bremen.
[10] H. Krag, J.S. Srinivas, A. Di Mira, I. Zayer, T. Flohrer, Ground-Based laser for Tracking and Remediation – an architectural view, IAC-18-A6.7.1, 69th International Astronautical Congress, Bremen, Germany, October 2018.
[11] C.R. Phipps, C. Bonnal, Using pulsed laser ranging to drastically improve LEO orbit ephemerii, #192, 8th EUCASS, Madrid, July 2019, https://doi.org/10.13009/EUCASS2019-192.
[12] C.R. Phipps, “L’ADROIT - a spaceborne ultraviolet laser system for space debris clearing, Acta Astronatica 104 (2014) 243–255.
[13] G. Sarver, C. Levit, Satellite debris removal mission, Proceedings of the International Conference on Orbital Debris Removal, Chantilly, USA, December 2009.
[14] D. McKnight, C. Bonnal, Options for generating JCA clouds, #8.5, Proceedings of the 4th Workshop on Modeling and Remediation, Paris, France, June 2016.
[15] C.R. Phipps, C. Bonnal, A spaceborne, pulsed UV laser for re-entering or nudging LEO debris, and re-orbiting GEO debris, Acta Astronaut. 118 (2016) 224–236, https://doi.org/10.1016/j.actaastro.2015.10.005.
[16] C.R. Phipps, C. Bonnal, F. Masson, Large debris traffic management (LDTM) using lasers, #7.6, Proceedings of the 5th Workshop on Modeling and Remediation, Paris, France, June 2018.
[17] S.A.E. Boyer, M. Boustie, L. Berthe, S. Baton, E. Brambrink, L. Videau, C. Rousseau, J.-M. Chevalier, C.R. Phipps, F. Masson, S. Oriol, C. Bonnal, New advances in short-pulse laser for LEO environment, #1062, 8th European Conference for Aeronautics and Space Sciences, Madrid 1-4 July, 2019.
[18] S.A.E. Boyer, A. Burr, S. Jacomet, M. Boustie, L. Berthe, S. Baton, E. Brambrink, L. Videau, J.-M. Chevalier, M. Schneider, C.R. Phipps, F. Masson, C. Bonnal, 400fs and 80ps pulse laser in selected materials: first in-situ and post-mortem analysis, International Conference on Processing and Manufacturing of Advanced Materials, Paris 9-13, July 2018.
[19] T. Ebisuzaki, et al., Deorbiting mission of cm-sized space debris by laser ablation, Paper 7.4, 5th European Workshop on Space Debris Modeling and Remediation, Paris, June 2018.
[20] IAA Space Debris Situation Report –, (2016) ISBN/EAN IAA: 978-2-917761-56-4 http://www.iaaweb.org/iaa/Scientific%20Activity/sg514finalreport.pdf.
[21] A. Jarry, C. Bonnal, C. Dupont, S. Missonnier, L. Lequette, F. Masson, SRM plume: a candidate as space debris braking system for Just-In-Time Collision avoidance maneuver, Acta Astronaut. 158 (2019) 185–197.
[22] C. Dupont, Missonnier, S. Rommelaere, C. Bonnal, Just-in-time Collision Avoidance mission: reactive system for braking space debris, 8th EUCASS, #724 July 2019, https://doi.org/10.13009/EUCASS2019-724 Madrid.
[23] R.F. Lark, Cryogenic Positive Expulsion Bladders” NASA-TM-X-1555, (April, 1968).
[24] Available at: http://www.space-propulsion.com/brochures/propellant-tanks/58lt-n2h4-bladder-tank-bt01-0.pdf.
[25] D. McKnight, F. Santoni, Bringing Massive Derelicts Back to Life, 17th Reinventing Space Conference BIS-RS-2019-01, Belfast, (November 2019).
[26] D. McKnight, F. Di Pentino, Kaczmarek, S. Knowles, Detumbling rocket bodies in preparation for active debris removal, Proceedings 7th European on Space Debris, Darmstadt, Germany, April 2013.
[27] http://www.cs.cmu.edu/~msitti/papers/nature00.pdf.
[28] T. Brian, T. McLeod, L. Gagliano, Innovative electrostatic adhesion technologies (flexible electrostatic tools for capture & handling [FETCH]), #6.2, Proceedings of the 4th Workshop on Modeling and Remediation, Paris, France, June 2016.
[29] http://www.busek.com/index_htm_files/70000700A%20BHT-200.pdf.